Observing Trajectories with Weak Measurements in Quantum Systems in the Semiclassical Regime

A. Matzkin

LPTM, CNRS Unité 8089, Université de Cergy-Pontoise, 95302 Cergy-Pontoise cedex, France
(Received 2 March 2012; published 10 October 2012)

We propose a scheme allowing us to observe the evolution of a quantum system in the semiclassical regime along the paths generated by the propagator. The scheme relies on performing consecutive weak measurements of the position. We show how "weak trajectories" can be extracted from the pointers of a series of devices having weakly interacted with the system. The properties of these weak trajectories are investigated and illustrated in the case of a time-dependent model system.

In classical physics, the evolution of a physical system is given in terms of trajectories. Instead, quantum mechanics forbids a fundamental description based on trajectories. Nevertheless, the Feynman path integral approach gives a sum over paths formulation of the evolution of a quantum system, and when the actions are large relative to $\hbar$—the semiclassical regime–, the wave function evolves essentially along classical paths, those of the corresponding classical system [1]. Of course, this does not mean that a quantum object is a localized particle moving on a definite path. But trajectories may remain significant in quantum systems: the large scale properties, experimentally observed in many systems [1,2], display the *signatures* of the underlying classical dynamics.

In this work, we aim to go further by proposing a scheme allowing us to observe the evolution of a quantum system in the semiclassical regime along the trajectories of the corresponding classical system. The scheme relies on performing consecutive weak measurements (WM). WM [3,4] are characterized by a very weak coupling between the system and the measurement apparatus. Thus measuring weakly an observable $\hat{A}$ results in leaving the former essentially unperturbed while the latter picks up on average a limited amount of information encapsulated in the weak value (WV)

$$\langle\hat{A}\rangle_W = \frac{\langle\chi|\hat{A}|\psi\rangle}{\langle\chi|\psi\rangle}; \qquad (1)$$

$|\psi\rangle$ is the initial (preselected) state and $\langle\chi|$ is the final (postselected) state obtained by performing a standard strong measurement after having measured $\hat{A}$ weakly. WM are receiving increased attention, either as a technique for signal amplification [5] or as a tool to investigate fundamental problems, from a theoretical standpoint but also experimentally [6]. In particular, in a beautiful recent experiment [7] nonclassical "average trajectories" (AT) for photons deduced indirectly from the WM of momentum have been observed. In our scheme we introduce instead weak trajectories (WT) by measuring *directly* the

position of a quantum system interacting weakly with a set of meters. We will see that in the semiclassical regime the only WT compatible with the positions of the pointers are the classical paths.

Let $|\psi(t_i)\rangle$ be the initial state of a dynamical system whose evolution is governed by a (possibly time-dependent) Hamiltonian $H(t)$. Let us introduce a meter consisting of a particle positioned at $\mathbf{R}_\kappa^0$. Its spatial wave function $\langle\mathbf{R}_\kappa|\phi_\kappa\rangle$, assumed to be tightly localized around $\mathbf{R}_\kappa^0$ acts as pointer. For convenience the wave function can be taken to be a Gaussian, $\langle\mathbf{R}_\kappa|\phi_\kappa\rangle = (2/\pi\Delta^2)^{1/2}e^{-(\mathbf{R}_\kappa-\mathbf{R}_\kappa^0)^2/\Delta^2}$ (we work from now on in a 2D configuration space and use atomic units throughout). The local coupling between the meter and the system is assumed to take place during a small time interval τ, triggered when the system and pointer wave functions overlap. The time-integrated interaction is taken as $I_\kappa = g\mathbf{r}\cdot\mathbf{R}_\kappa\theta((4\Delta)^2 - |\mathbf{r} - \mathbf{R}_\kappa|^2)$, where g is the effective coupling strength and the last term is a unit-step function accounting for the short range character of the interaction (this term will be implicit in the rest of the Letter). Assume now we have a set of meters $\kappa = 1, ..., n$ positioned at $\mathbf{R}_\kappa^0$. Let t_κ denote the mean interaction time of the κth pointer with the system. The initial state of the system and meters $|\Psi(t_i)\rangle = |\psi(t_i)\rangle\prod_{\kappa=1}^n|\phi_\kappa\rangle$ evolves at time t_f to [8]

$$|\Psi(t_f)\rangle = U(t_f, t_n)e^{-iI_n}U(t_n, t_{n-1})...e^{-iI_1}U(t_1, t_i)|\Psi(t_i)\rangle, \qquad (2)$$

where $U(t_{k+1}, t_k)$ denotes the unitary self evolution of the system between two interactions; k relabels the meters according to the order in which they interact with the system.

At time t_f a standard projective measurement is made in order to postselect the system to a desired final state $|\chi(t_f)\rangle$. Expanding each I_k in Eq. (2) to first order in the coupling g leads to

$$\prod_{k=1}^{n} \langle \mathbf{R}_k | \langle \chi(t_f) | \Psi(t_f) \rangle \simeq \langle \chi(t_f) | \psi(t_f) \rangle$$

$$\times \prod_{k=1}^{n} \exp[-ig\langle \mathbf{r}(t_k)\rangle_W \cdot \mathbf{R}_k]\phi_k(\mathbf{R}_k, \mathbf{R}_k^0), \quad (3)$$

where $\langle \mathbf{r}(t_k)\rangle_W$ is the weak value [Eq. (1)] given here by

$$\langle \mathbf{r}(t_k)\rangle_W \equiv \frac{\langle \chi(t_k) | \mathbf{r} | \psi(t_k)\rangle}{\langle \chi(t_k) | \psi(t_k)\rangle} \quad (4)$$

with $\mathbf{r} = x\hat{\mathbf{x}} + y\hat{\mathbf{y}}$. Equations (3) and (4) indicate that as a result of the interaction that took place at t_k, each meter wave function $\phi_k(\mathbf{R}_k, \mathbf{R}_k^0)$ will incur a phase shift given by the WV $\langle \mathbf{r}(t_k)\rangle_W$. As in the standard WM scenario [3], this phase shift appears as a shift in the momentum space wave function of each pointer. Since Eq. (3) holds provided g and Δ are very small, the momentum space wave functions will be broad, meaning a high number of events must be recorded in order to observe each shift.

The structure of $\langle \mathbf{r}(t_k)\rangle_W$ deserves a special comment. Each $\langle \mathbf{r}(t_k)\rangle_W$ is defined at $t = t_k$ with an effective preselected state $|\psi(t_k)\rangle = U(t_k, t_i)|\psi(t_i)\rangle$ being the initial state propagated *forward* in time and an effective postselected state $\langle \chi(t_k)| = \langle \chi(t_f)|U(t_f, t_k)$ being the postselected state evolved *backward* in time; this property illustrates the close relation between WM and time-symmetric formulations of quantum mechanics [4]. Note that contrary to the usual definition of weak values, the effective pre and postselected states defining $\langle \mathbf{r}(t_k)\rangle_W$ cannot be chosen: only the initial and the final states can be freely set. A WV at some intermediate time t_k reflects the interaction I_k with the kth meter given the unitary evolution of the preselected and postselected states of the system. We can therefore envisage the set $\{t_k, \langle \mathbf{r}(t_k)\rangle_W\}$ as defining a *weak trajectory* of the system evolving from an initial state to a final postselected state as recorded by the pointers positioned at $\mathbf{R}_k^0$, $k = 1, ..., n$.

For an arbitrary quantum system a WT will typically reflect the space-time correlation between the forward evolution of the preselected state and the backward evolution of the postselected state at the positions $\mathbf{R}_k^0$ of the weakly interacting meters. Although obtaining this type of information is certainly of interest in general quantum systems, the notion of weak trajectories is particularly suited to investigate the evolution of a quantum system in the semiclassical regime. In this regime a typical wave function evolves according to the asymptotic form of the path integral propagator [9],

$$\psi(\mathbf{r}, t) = \int d\mathbf{r}' \left(\sum_{cl} \frac{1}{(2i\pi\hbar)} \left| \det\frac{\partial^2 S_{cl}(\mathbf{r}, \mathbf{r}', t)}{\partial \mathbf{r} \partial \mathbf{r}'} \right|^{1/2} \right.$$

$$\left. \times \exp[iS_{cl}(\mathbf{r}, \mathbf{r}', t)/\hbar - i\mu_{cl}] \right) \psi(\mathbf{r}', 0), \quad (5)$$

where cl runs on the classical trajectories connecting $\mathbf{r}'$ to $\mathbf{r}$ in time t (from now on we set $t_i = 0$) and the term between the large parentheses is the semiclassical propagator obtained from the asymptotics ($S_{cl} \gg \hbar$) of the path integral form of the evolution operator $U(t, 0)$. S_{cl} is the classical action and μ_{cl} the topological index of each path. Working out the full semiclassical propagation is often a formidable task, especially as the number of trajectories proliferate in the regimes where the semiclassical approximation holds. However, if the initial state is well localized, the semiclassical propagation can be simplified by linearizing the action around an initial and a final reference point linked in time t by a central classical trajectory, the guiding trajectory [10]. Linearization is particularly relevant if $\psi(\mathbf{r}', 0)$ is chosen to be a localized Gaussian

$$\psi_{\mathbf{r}_0, \mathbf{p}_0}(\mathbf{r}', 0) = \left(\frac{2}{\pi\delta^2}\right)^{1/2} e^{-(\mathbf{r}'-\mathbf{r}_0)^2/\delta^2} e^{i\mathbf{p}_0 \cdot (\mathbf{r}'-\mathbf{r}_0)/\hbar}. \quad (6)$$

The initial reference point is the maximum of the Gaussian, the linearized action in Eq. (5) is a quadratic form, whereas the determinant prefactor becomes a purely time-dependent term that can be written in terms of the stability matrix of the guiding trajectory. This linearized information along the central reference trajectory effectively replaces the sum over cl.

The integral (5) can then be performed exactly: the result (often known as the thawed Gaussian approximation) is of the form [10]

$$\psi_{\mathbf{r}_0, \mathbf{p}_0}(\mathbf{r}, t) = \text{Tr}[\mathbf{A}(t)] e^{-(\mathbf{r}-\mathbf{q}(t)) \cdot [\mathbf{M}(t)+i\mathbf{N}(t)] \cdot (\mathbf{r}-\mathbf{q}(t))}$$

$$\times e^{i\mathbf{p}(t) \cdot (\mathbf{r}-\mathbf{q}(t))/\hbar} e^{iS_{cl}(\mathbf{q}(t),\mathbf{r}_0,t)/\hbar}, \quad (7)$$

where $(\mathbf{q}(t), \mathbf{p}(t))$ are the phase-space coordinates of the guiding classical trajectory with initial conditions $(\mathbf{r}_0, \mathbf{p}_0)$ and $\mathbf{A}$, $\mathbf{M}$ and $\mathbf{N}$ are time-dependent matrices depending solely on the stability elements of the guiding trajectory. The advantage of working in the linearized regime is that by picking a preselected state of the form

$$\langle \mathbf{r} | \psi(t_i)\rangle = \sum_j c_j \psi_{\mathbf{r}_0, \mathbf{p}_j}(\mathbf{r}, t_i), \quad (8)$$

i.e., a superposition of Gaussians (6) launched in different directions $\mathbf{p}_j$, one is dealing conceptually with the type of problem defined by the semiclassical propagation (5) with a simplified and perfectly controlled dynamics. The evolution operator $U(t_1, t_i)$ of Eq. (2) propagates each term of Eq. (8) along the relevant guiding trajectory yielding at t_1 the superposition of evolved states $\sum_j c_j \psi_{\mathbf{r}_0, \mathbf{p}_j}(\mathbf{r}, t_1)$, each state being given by Eq. (7) (recall that $\mathbf{q}$, $\mathbf{p}$, and the matrices $\mathbf{A}$, $\mathbf{M}$, and $\mathbf{N}$ explicitly depend on j).

The postselected state will also be taken to be a Gaussian of the type (6) localized in the vicinity of a chosen point $\mathbf{r}_f$ at time t_f

$$\chi_{\mathbf{r}_f, \mathbf{p}_f}(\mathbf{r}, t_f) = \left(\frac{2}{\pi\delta_f^2}\right)^{1/2} e^{-(\mathbf{r}-\mathbf{r}_f)^2/\delta_f^2} e^{i\mathbf{p}_f \cdot (\mathbf{r}-\mathbf{r}_f)/\hbar}. \quad (9)$$

In the linearized approximation, finding the backward propagated state is tantamount to obtaining the *unique* solution of the form (7) such that $\psi_{\mathbf{r}(t_1),\mathbf{p}(t_1)}(\mathbf{r}, t_f) = \chi_{\mathbf{r}_f,\mathbf{p}_f}(\mathbf{r}, t_f)$: this gives a wave function centered on a time-reversed classical trajectory having boundary conditions $(\mathbf{r}_f, \mathbf{p}_f)$ at $t = t_f$ and position $\mathbf{q}_f(t_k)$ at $t = t_k$. Assume the meters lie at positions $\mathbf{R}_k^0$ where the overlap between the different branches of the system wave function (8) is negligible. The weak values (4) can then be computed exactly: if $\psi_{\mathbf{r}_0,\mathbf{p}_j}(\mathbf{r}, t_k)$ (for all j) or $\chi_{\mathbf{r}_f,\mathbf{p}_f}(\mathbf{r}, t_k)$ vanish in the vicinity of $\mathbf{R}_k^0$ the meter does not move: there is no weak trajectory in the neighborhood of this point. Otherwise, $\chi_{\mathbf{r}_f,\mathbf{p}_f}(\mathbf{r}, t_k)$ overlaps at most with one branch, say $\psi_{\mathbf{r}_0,\mathbf{p}_J}$; denoting the distance between the maxima of the wave packet and of the postselected state at $t = t_k$ by $\boldsymbol{\epsilon}_k = \mathbf{q}_J(t_k) - \mathbf{q}_f(t_k)$, the WV $\langle \mathbf{r}(t_k) \rangle_W = \langle x(t_k) \rangle_W \hat{\mathbf{x}} + \langle y(t_k) \rangle_W \hat{\mathbf{y}}$ takes the form

$$\langle x(t_k) \rangle_W = [\mathbf{q}_J(t_k) \cdot \hat{\mathbf{x}} + a_x \boldsymbol{\epsilon}_k \cdot \hat{\mathbf{x}} + b_x (\mathbf{p}_J(t_k) - \mathbf{p}_f(t_k)) \cdot \hat{\mathbf{x}}]$$
$$+ i[g_x(t_k)\boldsymbol{\epsilon}_k \cdot \hat{\mathbf{x}} + h_x(\mathbf{p}_J(t_k) - \mathbf{p}_f(t_k)) \cdot \hat{\mathbf{x}}], \quad (10)$$

and analog expressions for $\langle y(t_k) \rangle_W$. a, b, g, and h are time-dependent functions whose explicit forms are cumbersome though straightforward to evaluate.

The structure of Eq. (10) emphasizes the special role of the postselected state with $(\mathbf{r}_f, \mathbf{p}_f)$ chosen such that the backward evolved trajectory simply retraces the guiding trajectory $\mathbf{q}_J(t)$. For this special choice $\boldsymbol{\epsilon}_k = 0$ and $\mathbf{p}_J(t_k) = \mathbf{p}_f(t_k)$ for any value of t_k. If n meters happen to be in regions where χ and ψ_J overlap *each* of these meters will record $\langle \mathbf{r}(t_k) \rangle_W = \mathbf{q}_J(t_k)$, i.e., the position of the underlying classical trajectory. The WT $\{t_k, \langle \mathbf{r}(t_k) \rangle_W\}$ thus corresponds to the guiding trajectory of the linearized Feynman propagator. For any other choice of postselection $\langle \mathbf{r}(t_k) \rangle_W$ (where defined) will yield a complex number, with the real part indicating a registered position that will be markedly different from the average position of the wave packet. The imaginary part of Eq. (10) does not inform on the value of the weakly measured observable (as is the rule for any WV) but is related to the average backaction induced on the weak meter by the postselection [11].

For the purpose of illustration—and to avoid spurious effects due to the quality of the linearized approximation—we will take a 2D time-dependent linear oscillator (TDLO). The linearized propagator for the TDLO is quantum mechanically exact, while the varying amplitudes capture many features of semiclassical systems with more involved dynamics. The TDLO is often employed to model diverse systems, like ions in a trap [12]. The Hamiltonian for the system is $H = (P_x^2 + P_y^2)/2m + mV_x(t)x^2 + mV_y(t)y^2$, where for definiteness we choose $V_i(t) = \xi_i - \upsilon_i \cos(2\omega_i t)$ ($i = x, y$; ξ, υ and ω are constants). The wave function (7) is obtained directly by employing standard path integral techniques [9]; the classical trajectories can be found in closed form from the

solutions of Ermakov systems [13]. The preselected state (8) is taken as the superposition of 3 Gaussians at the origin with mean momenta as shown in Fig. 1(a). The maximum of each wave packet then evolves by following the guiding trajectory, *I*, *II*, or *III* shown in Fig. 1.

Let us first set the postselected state (9) with $\mathbf{r}_f = \mathbf{q}_I(t_f)$ and $\mathbf{p}_f = \mathbf{p}_I(t_f)$ and let us position the meters $\mathcal{D}_k$ as shown in Fig. 2(a). The backward evolution of $|\chi(t_f)\rangle$ simply retraces trajectory *I* backwards. Therefore, the pointer in $\mathcal{D}_3$ displays according to Eq. (10) the position $\mathbf{q}_I(t_3)$ while $\mathcal{D}_2$ and $\mathcal{D}_1$ do not move at all (no overlap with $|\chi(t)\rangle$ at any t). One concludes that the particle went through $\mathcal{D}_3$ but not through $\mathcal{D}_1$ and $\mathcal{D}_2$. If instead of $\mathcal{D}_1$ and $\mathcal{D}_2$ other meters $\mathcal{D}_1'$ and $\mathcal{D}_2'$ positioned as shown in Fig. 3(a) are employed, then these pointers display, respectively, the WV $\mathbf{q}_I(t_1)$ and $\mathbf{q}_I(t_2)$: the particle went through $\mathcal{D}_1'$, $\mathcal{D}_2'$, and $\mathcal{D}_3$. Hence, one concludes (possibly by inserting additional devices) that the particle took the WT defined by the classical trajectory *I*. Note that according to Eq. (10) there is no quantum state of the form (9) that can yield a WT going through $\mathcal{D}_1$, $\mathcal{D}_2$, and $\mathcal{D}_3$. This is due to the fact, implied by the propagator (5), that there does not exist a wave packet arriving in the neighborhood of $\mathbf{r}_f$ at time t_f that would have previously visited the neighborhoods of $\mathcal{D}_1$, $\mathcal{D}_2$, and $\mathcal{D}_3$.
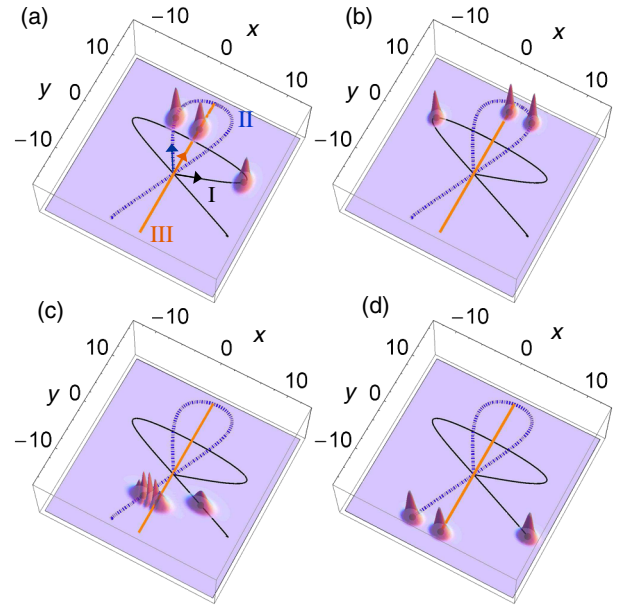

FIG. 1 (color online). Time evolution of the wave function initially ($t_i = 0$) given by Eq. (8) with $\mathbf{r}_0 = \mathbf{0}$ and the initial mean momenta $\mathbf{p}_j$, $j = I, II, III$ taken as indicated by the arrows in panel (a). The reference classical trajectories *I*, *II* and *III* are shown, respectively, in black, dashed blue, and orange. (a) The wave function at $t_1 = 0.7$, (b) at $t_2 = 2$, (c) at $t_3 = 3.15$ (after the wave packets cross the origin), and (d) at $t_f = 3.65$, the time at which postselection is made.
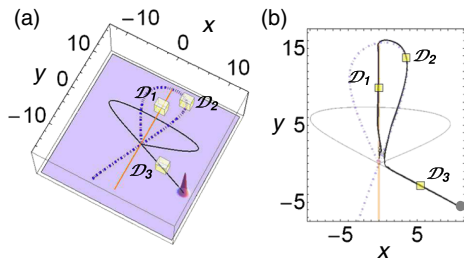
FIG. 2 (color online). (a) The postselected wave function, a Gaussian localized on the guiding trajectory *I*, is shown, along with the positions of the meters $\mathcal{D}_{1,2,3}$. Only the pointer $\mathcal{D}_3$ is affected, while $\mathcal{D}_{1,2}$ remain still: there is no WT joining the corresponding positions. (b) The average trajectories obtained from WM of the *momentum* are plotted in solid black: 9 trajectories having their final positions on and near the maximum of the postselected state are shown, along with the reference trajectories (in faded colors).

The last remark highlights the incompatibility between the weak trajectories defined here by consecutive WM of the position and the average trajectories defined by a WM of the *momentum* immediately postselected to a given position. By repeating these weak momentum measurements for different postselected positions, a velocity field is obtained. The AT are precisely the trajectories built on this velocity field. They have been experimentally observed recently for photons in a double slit setup [7]. It was previously known [14] that their dynamics is governed by the law of motion of the de Broglie–Bohm theory [15], i.e., by the probability flow, whereas the WT are generated by the semiclassical propagator (5). The mismatch [16] between de Broglie–Bohm and classical trajectories in semiclassical systems hinges on the fact that when wave packets interfere, the overall mean velocity field differs from the group velocity of each individual wave packet.
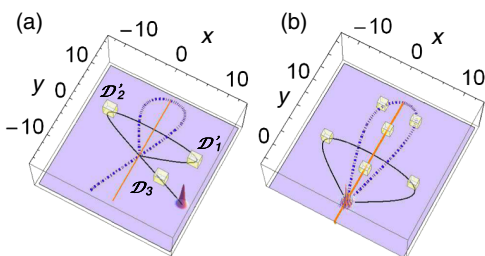

FIG. 3 (color online). (a) The postselected wave function (the same as displayed in Fig. 2) is shown with the meters $\mathcal{D}'_1$, $\mathcal{D}'_2$, and $\mathcal{D}_3$. Each of these pointers indicates a weak value $\mathbf{q}_I(t_k)$: the evolution of the system along the reference trajectory *I* has been measured weakly. (b) Postselection now takes places at $t_O = 2.84$ when the wave packets return simultaneously to the origin. The postselected state (defined in the text) is plotted along with the pointers positioned along the reference trajectories *I*, *II*, *III*. *All* the meters yield weak values in agreement with their position along the relevant classical trajectory: the semiclassical sum over paths formulation has thus been measured weakly.

The mismatch is illustrated here in Fig. 2(b): we have computed numerically [8] several AT arriving in the neighborhood of $\mathbf{r}_f = \mathbf{q}_I(t_f)$. These AT go indeed through $\mathcal{D}_1$, $\mathcal{D}_2$, and $\mathcal{D}_3$: starting near the origin, they first move in the vicinity of the guiding trajectory *III*, then travel along trajectory *II* and, thereafter, jump so as to move along trajectory *I*.

Finally, consider choosing postselection at $t_f = t_O$ when trajectories *I*, *II*, and *III* first return to the origin, with the postselected state chosen as the superposition $\chi_O(\mathbf{r}, t_O) = \sum_j \chi_{\mathbf{r}_f=0,\mathbf{p}_{O_j}}(\mathbf{r}, t_O)$, with $\chi_{\mathbf{r}_f=0,\mathbf{p}_{O_j}}$ given by Eq. (9) and $\mathbf{p}_{O_j} = \mathbf{p}_j(t_O)$, $j = I, II, III$. Several pointers are positioned as shown in Fig. 3(b). By construction the backward evolution of χ_O yields a superposition of wave packets retracing trajectories *I*, *II*, and *III* respectively. Therefore, *all* the pointers will display a WV consistent with their position along one of the three trajectories, indicating the particle was there. This is an experimentally realizable way to catch the essence of the path integral approach in the semiclassical regime: weakly interacting meters indicate the "particle" takes *simultaneously* all the available classical paths. In contrast a strong projective measurement would of course yield a definite outcome on only *one* of the paths.

To sum up, we have defined weak trajectories allowing us to observe the paths taken by a quantum system in the semiclassical regime by direct weak measurements of the position. A consequence worth exploring concerns the possibility of employing this scheme to reconstruct the unknown propagator of a semiclassical system from the observed WT obtained from a grid of weak detectors while filtering postselected states. Possible experimental realizations could be considered in systems in which wave packets with a controlled dynamics can be engineered [17]. The present setup may also be used in designing pre-postselected quantum paradoxes containing dynamical ingredients.

[1] M. Brack and R Bhaduri, *Semiclassical Physics* (Westview, Boulder, 1997).

[2] M. R. Haggerty, N. Spellmeyer, D. Kleppner, and J. Delos, Phys. Rev. Lett. **81**, 1592 (1998); A. Matzkin, M. Raoult, and D. Gauyacq, Phys. Rev. A **68**, 061401(R) (2003); Z. Chen, W. Zhou, B. Zhang, C. Yu, J. Zhu, W. Lu, and S. Shen, Phys. Rev. Lett. **102**, 244103 (2009); J. D. Wright, J. M. DiSciacca, J. M. Lambert, and T. J. Morgan, Phys. Rev. A **81**, 063409 (2010).

[3] Y. Aharonov, D. Albert, and L. Vaidman, Phys. Rev. Lett. **60**, 1351 (1988).

[4] Y. Aharonov, S. Popescu, and J. Tollaksen, Phys. Today **63**, No. 11, 27 (2010).

[5] O. Hosten and P. Kwiat, Science **319**, 787 (2008); P. B. Dixon, D. Starling, A. Jordan, and J. Howell, Phys. Rev. Lett. **102**, 173601 (2009).

[6] See, e.g., Y. Aharonov and A. Botero, Phys. Rev. A **72**, 052111 (2005); G. Mitchison, R. Jozsa, and S. Popescu, Phys. Rev. A **76**, 062105 (2007); J. S. Lundeen and A. M. Steinberg, Phys. Rev. Lett. **102**, 020404 (2009); A. Tanaka, Phys. Lett. A **297**, 307 (2002); Y. Kedem and L. Vaidman, Phys. Rev. Lett. **105**, 230401 (2010); M. Iinuma, Y. Suzuki, G. Taguchi, Y. Kadoya, and H. F. Hofmann, New J. Phys. **13**, 033041 (2011); M. E. Goggin, M. P. Almeida, M. Barbieri, B. P. Lanyon, J. L. O'Brien, A. G. White, and G. J. Pryde, Proc. Natl. Acad. Sci. U.S.A. **108**, 1256 (2011).

[7] Kocsis, B. Braverman, S. Ravets, M. J. Stevens, R. P. Mirin, L. K. Shalm, and A. M. Steinberg, Science **332**, 1170 (2011).

[8] See Supplemental Material at http://link.aps.org/supplemental/10.1103/PhysRevLett.109.150407 for details.

[9] L. S. Schulman, *Techniques and Applications of Path Integration* (Wiley, New York, 1996).

[10] E. J. Heller, in *Chaos and Quantum Physics* (Elsevier, Amsterdam, 1991), Chap. 9.

[11] A. M. Steinberg, Phys. Rev. Lett. **74**, 2405 (1995); J. Dressel and A. N. Jordan, Phys. Rev. A **85**, 012107 (2012).

[12] N. C. Menicucci and G. J. Milburn, Phys. Rev. A **76**, 052105 (2007).

[13] A. K. Dhara and S. V. Lawande, Phys. Rev. A **30**, 560 (1984).

[14] H. Wiseman, New J. Phys. **9**, 165 (2007).

[15] D. Bohm and B. J. Hiley, *The Undivided Universe* (Routledge, London, 1993).

[16] A. Matzkin, Found. Phys. **39**, 903 (2009).

[17] J. J. Mestayer, W. Zhao, J. Lancaster, F. Dunning, C. Reinhold, S. Yoshida, and J. Burgdörfer, Phys. Rev. Lett. **99**, 183003 (2007); A. Buchleitner, D. Delande, and J. Zakrzewski, Phys. Rep. **368**, 409 (2002).